EVS24
Stavanger, Norway, May 13-16, 2009

Parameter Prediction and Modelling Methods for Traction Motor of Hybrid Electric Vehicle

Tao Sun, Soon-O Kwon, Geun-Ho Lee, Jung-Pyo Hong

Department of Automotive Engineering, Hanyang University, Seoul, 133791, Korea, hongjp@hanyang.ac.kr

Abstract

This paper introduces the parameter prediction and modelling methods for the traction motor of hybrid electric vehicle (HEV). In the general HEV simulation, the traction motor is mainly defined by efficiency map and torque/speed curve. Therefore, this paper will focus on the prediction of these parameters, which involves the numerical analysis on the motor inductances calculation, iron-loss resistance calculation, and characteristic estimation algorithm and so on. The modelling method is split into tow major parts: configuration of model and composing graphic user interface (GUI). An experiment result will be used to compare with the calculated efficiency map to verify the validity of these methods. In addition, the model construction will be explained by flowcharts. Considering popularity, the MATLAB/Simulink will be used to construct the simulation program. And a GUI will be designed and used to show the simulation results. With the other models of vehicle components, the simulation will be processed in a parallel-type HEV model in an urban road condition (FTP72), and the simulation results will be shown in the end of this paper.

Keywords: Hybrid Electric Vehicle, Modelling, Interior Permanent Magnet Synchronous Motor, Motor Characteristic

1 Introduction

Since the Toyota-Prius and Honda-Insight achieve great success in the both environment and economic issues, most of automotive companies have paid much attention on the development of hybrid electric vehicle (HEV) in global. Due to the extra traction motor, the integrate traction system of HEV becomes more complex than that of traditional vehicle. It is not only difficult to design the control algorithm of HEV, but also hard to determine the specification of each component and estimate the overall performance [1] [2]. Based on these problems, it is necessary to develop a HEV simulator in software for testing the prototype design before manufacturing. Due to the great difference between the electrical time constant and

mechanical time constant, the time consuming transient simulation is not necessary. Thus, the general HEV simulator is usually composed by steady-state date lookup table [1]. As one part of this simulator, fundamentally, the traction motor model should be able to generate accurate input and/or output torque, input and/or output electric power, and own efficiency, which implies the steady-state efficiency map data and torque/speed curve data are basically required.

Because of many prevalence, the interior permanent magnet synchronous motor (IPMSM) has been successfully used in Prius, hybrid Civic and other commercial hybrid vehicles. Therefore, this paper will focus on the calculation of the lookup table data of the IPMSM, which will involved the parameter prediction for the nonlinear inductances, iron-loss resistance, and character-istics analysis of IPMSM. And considering the

popularity, using the calculated characteristics data, the motor model will be established in MATLAB/Simulnk, and the detail configuration of model will be explained in flowcharts. In order to give convenience to the users, a graphic user interface (GUI) is designed. Finally, the calculated efficiency map data will be verified by the experiment data. And this motor model will be processed with the models of the other HEV components in a parallel-type HEV model in an urban road condition (FTP72). The simulation results will be shown in the end of this paper.

2 Determination of Parameters

In many successful commercial products of HEV, the traction motor is chosen as IPMSM because it has many advantages, such as high power density, wide speed range, and high efficiency [5]. Therefore, this paper adopts an IPMSM as the analysis model. The specification of this motor is shown in Table 1. And its cross-section is shown in Figure. 1.

Table I: Specifications of IPMSM

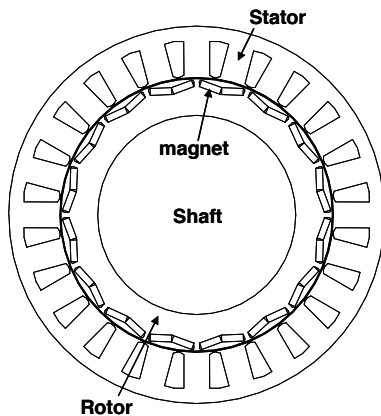| parameters	Values	
stator outer diameter	270.0	mm
rotor outer diameter	198.0	mm
rotor stack length	35.0	mm
air gap length	0.9	mm
size of magnet	14.2x4.8x35	mm^3
number of poles/ slots	16 / 24	-
DC link Voltage	130	V
material of iron	S18	-

Figure 1: Cross-section of Analysis IPMSM

According to the Park transformation, the 3-phase AC motor usually is transformed to 2-phase dq-axis model. The equations of IPMSM in the synchronous dq reference of frame are ex-pressed in (1)-(3) [3].

$$\begin{bmatrix} v_d \\ v_q \end{bmatrix} = R_a \begin{bmatrix} i_{od} \\ i_{oq} \end{bmatrix} + \left(1 + \frac{R_a}{R_c}\right)\begin{bmatrix} v_{od} \\ v_{oq} \end{bmatrix} + p\begin{bmatrix} L_d & 0 \\ 0 & L_q \end{bmatrix}\begin{bmatrix} i_{od} \\ i_{oq} \end{bmatrix}$$

(1)

$$\begin{bmatrix} v_{od} \\ v_{oq} \end{bmatrix} = \begin{bmatrix} 0 & -\omega L_q \\ \omega L_d & 0 \end{bmatrix}\begin{bmatrix} i_{od} \\ i_{oq} \end{bmatrix} + \begin{bmatrix} 0 \\ \omega \psi_a \end{bmatrix}$$

(2)

$$T = P\left[\psi_a i_{od} + \left(L_d - L_q\right)i_{od}i_{oq}\right]$$

(3)

where R_a: phase winding resistance,
R_c: resistance of iron losses,
L_d: d-axis inductance,
L_q: q-axis inductance,
P: number of pole pair,
ω: electrical angular velocity,
ψ_a: flux linkage of permanent magnet,
ψ_o: combined flux linkage of permanent magnet and excited winding,
i_{od}: d-axis load current,
i_{oq}: q-axis load current.

Additionally, the copper losses, iron losses, mechanical loss and efficiency can be calculated by (4), (5), (6) and (7).

$$P_c = R_a I_a{}^2 = R_a (i_d{}^2 + i_q{}^2)$$

(4)

$$P_i = \frac{V_o{}^2}{R_c} = \frac{\omega^2\left[(L_d i_{od} + \psi_a)^2 + (L_q i_{oq})^2\right]}{R_c}$$

(5)

$$P_m = P_w + P_f = 2D^2 Ln^3 \times 10^{-3} + K_f Mn^3 \times 10^{-3}$$

(6)

$$\eta = \frac{T \cdot \omega}{T \cdot \omega + P_c + P_i + P_m}$$

(7)

where P_c: copper losses,
P_i: iron losses,
P_m: mechanical losses,
P_w: windage loss,
P_f: bearing friction loss,
D: outer radii of rotor,
L: stack length of motor,
n: rotation angular velocity,
K_f: friction factor (1~3),
M: mass of rotor.

It can be seen that the four important parameters can affect the IPMSM voltage and current and hence, affect the each losses and efficiency. They are ψ_a, L_d and L_q, R_a and R_c. The ψ_a can be easily obtained from magneto-static finite elements analysis (FEA) [4]. The R_a can be calculated by the winding configuration and conductivity. However, the L_d, L_q and R_c are significant nonlinear variables. It is very difficult to determine them by analytical calculation. The following numerical techniques will be used to calculate them.

2.1 dq-axis inductances calculation

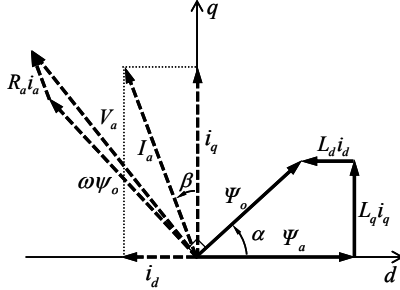The phasor diagram of IPMSM in steady state which ignored R_c is shown in Figure 2.

Figure 2: Phasor diagram of IPMSM in steady state

In the solid-line part, it can be seen that there are the relationships as described in (7) and (8).

$$L_d = \frac{\psi_0 \cos\alpha - \psi_a}{i_d} \qquad (7)$$

$$L_q = \frac{\psi_0 \sin\alpha}{i_q} \qquad (8)$$

And based on these two equations, the d- and q-axis inductance calculation process is described in Figure 3.
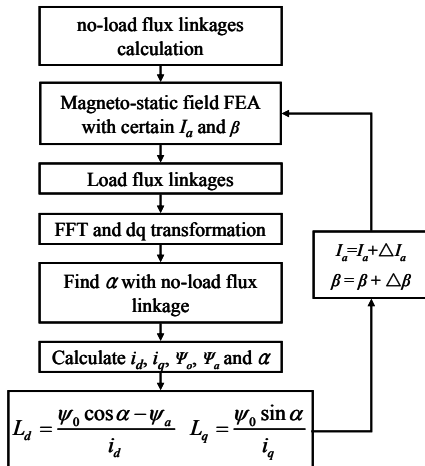

Figure 3: Process of inductance calculation method

2.2 Iron-loss resistance calculation

The dominant losses in IPMSM usually consist of copper loss, iron loss and mechanical loss. The copper loss is determined by winding resistance which is constant in a given temperature. The mechanical losses can be easily calculated by (6) according to known speed. The general expression of iron losses which include the hysteresis loss P_h, eddy current loss P_e and a anomalous component P_a is shown in (9) [4]

$$P_c = P_h + P_e + P_a = k_h f B_m^\alpha + k_e f^2 B_m^2 + k_a f^{1.5} B^{1.5} \qquad (9)$$

where the coefficients k_h, k_e, k_a and α are the function of frequency and amplitude of flux density. In addition, only sinusoidal variable is suitable for this formula. In practice, the flux density special and temporal distributions may be distorted. In this paper, a method which was proposed and verified in [5] is used to calculate the iron losses. It is described in Figure 4.
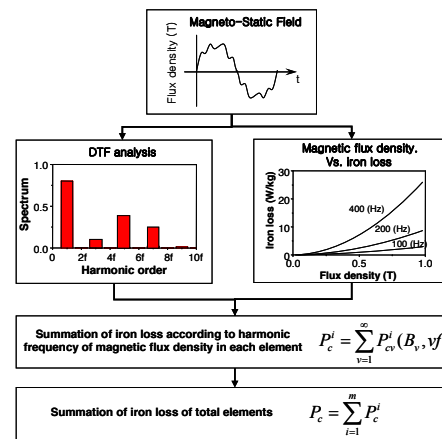

Figure 4: Process of iron-loss resistance calculation

2.2.1 Magneto-static field FEA

The 2D magneto-static field FEM is used to calculate the magnetic field distribution with the known current waveforms and time steps. Its governing equation, i.e. the nonlinear Possion equation, is described in (10).

$$\nabla \times \upsilon (\nabla \times A) = J + \nabla \times (\upsilon \mu_0 M) \qquad (10)$$

where A: magnetic potential vector,
    J: current density vector,
    M: magnetization vector,
    υ: reluctivity,
    μ_0: permeability of air.

2.2.2 Harmonics analysis

After obtain the flux density of each element, the frequency and amplitude of each harmonic component should be analyzed. In this paper, the Discrete Fourier Transform (DFT) is used. It can be expressed as

$$B_{pk}(k) = \sum_{n=0}^{N-1} B_p(n) e^{j(2\pi nk)/N} \qquad (11)$$

where k: harmonic order,

        N: number of the discrete data,

        $B_{pk}(k)$: amplitude of magnetic flux density of the kth harmonic,

        $B_p(n)$: magnitude of the point n (n=0, 1, …,N-1)

When the frequencies and amplitudes of magnetic flux density at each element are obtained, depending on them, the iron losses at each element are calculated from an iron loss data sheet that is tested by the Epstein test apparatus. Then, sum the results of all harmonics and all elements, the total iron loss can be obtained.

2.2.3   Equivalent iron-loss resistance

At the end, the equivalent iron-loss resistance is calculated by (12)

$$R_c = \frac{v_0^2}{P_c} \qquad (12)$$

where v_0 is the terminal voltage at base speed and no-load condition. And the iron loss resistance is 36.5 Ohm in this calculation.

2.3   Characteristics analysis

The IPMSM using in traction system usually is operated in Maximum Torque per Ampere (MTPA) control and flux weakening control. Although there is the corresponding equation for each control method [3], the characteristic analysis is much difficult to be done with it due to the nonlinear inductances and iron-loss resistance. This paper proposes a computer aided method which uses the iteration computation and loop condition to calculate the motor characteristics. Before the base speed, the loop condition is the maximum torque and current due to MTPA control. And after base speed, the maximum power or voltage is the loop condition. Once loop condition is satisfied, the calculated data is stored. The detail process is shown in Figure 5. By means of this method, the maximum torque/speed curve, efficiency map and any other characteristic data can be obtained.

3   Configuration of Model

Using the obtained efficiency map and maximum torque/speed curve data, a motor model is established in MATLAB/Simulink. This model accepts the switching-on (-off) and load signal from hybrid control unit (HCU), and index the available torque according to the feedback speed. This speed is calculated by generated torque and

motor moment of inertia. It is notable that at the first calculation step, the speed is zero. And this zero speed can index the maximum motor/generator torque. The motoring state or generating state is decided by the load signal which has range from 100% to -100%. After produce the torque and speed, the efficiency then can be indexed from the efficiency lookup table in speed and torque reference of frame. And according to (13) and (14), the electric power to battery is calculated at motoring and generating states.

Motoring state:

$$P_{electric} = P_{input} = P_{output} \div Efficiency \qquad (13)$$

Generating state:

$$P_{electric} = P_{output} = P_{input} \times Efficiency \qquad (14)$$

where the output power, P_{output}, in motoring state and input power, P_{input}, in generating state are calculated by the product of torque and speed. Thus, all the mechanical output in motoring state, and electric power to battery in motoring/generating states are solved in motor model. The flowchart of overview process is shown in Fig. 6.
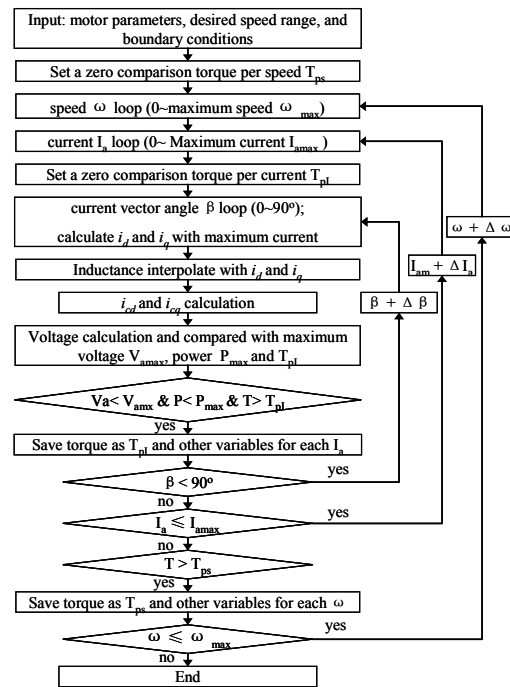

Figure 5: Data flowchart of characteristic analysis

4   Composing GUI

The raw program usually is not convenient for new user, particularly, when the input data is complex vector or map rather than one constant value. It is prefer to directly show the data in curve or figure.
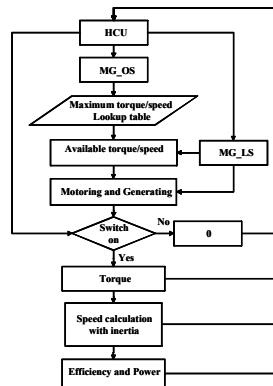
Figure 6: Data flowchart of motor model

In addition, in order to clearly show and analyze the simulation results, several results and even their combinations should be exhibited. At this time, the GUI gives a solution for these problems. As shown in Figure. 8, it is divided into data pre-view function and simulation results post-view function. The input data pre-view function can show the torque/speed curve and efficiency map. The other key parameter, moment of inertia, also can be changed in this window easily. The simulation results post-view function can show the torque distribution in efficiency map, efficiency distribution in whole operation range, and torque, speed and efficiency with time axis. These presentation methods will give much convenience to user so that they do not need to collect data and draw the figure by other software tools. Both time and economic benefits are achieved synchronously.
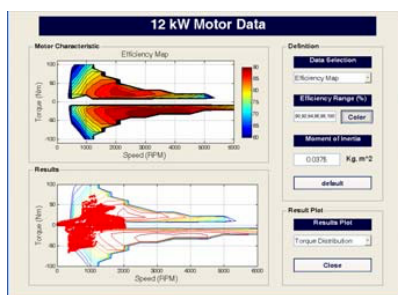

Figure 8: GUI of motor model

5   Results and Discussion

Fig. 9 shows the calculated d- and q-axis inductances profiles. It is obvious that the L_d has not much change in total current distribution, while the L_q behaves significant nonlinearity and saturation with the variation of i_d and i_q. Fig. 10 shows the characteristics of this IPMSM. The

efficiency map calculated by the proposed method is shown in Fig. 11 (a). Fig. 11 (b) shows the measured efficiency. It can be seen that the efficiency values and distributions of these two maps are quite similar.

The developed motor model is combined in a parallel type HEV simulator. As shown in Fig. 12, it consists of a Ni-MH battery, a 2.0 Liter diesel engine, a clutch and a two-simple 4 speed transmission. The simulation condition is with 1758 kg car mass, 2.28 m^2 front area, and 0.294 aero drag factor. The road condition is chosen as FTP72, the federal test procedure 72. All the mentioned simulation results are shown in Fig. 13 (a), (b) and (c). In the Torque distribution figure, i.e. Figure 13 (a), it can be seen that the motor mostly operates at low speed. And almost half and half torque distribution on the motoring mode and generating mode, respectively. This is mainly because of the maximum SOC control strategy.

6   Conclusion

This paper introduced an entire procedure to establish a motor model for the traction motor of HEV simulator. This procedure includes the prediction of parameters, configuration of model, and GUI. Following this procedure, a motor model is developed and tested in a parallel type HEV simulator. According to the simulation results, most necessary results can be simulated and easily observed in GUI window. In the further plan, the simulation validity will be verified by the commercial program and experiments.
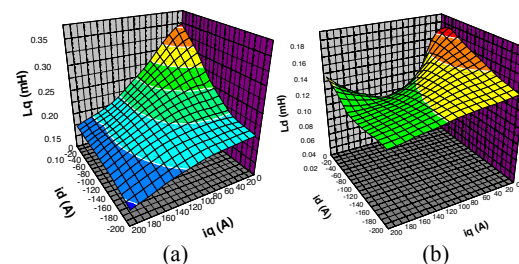

(a)   (b)

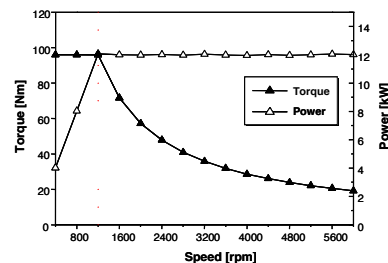Figure 9: (a) q-axis inductance, (b) d-axis inductance

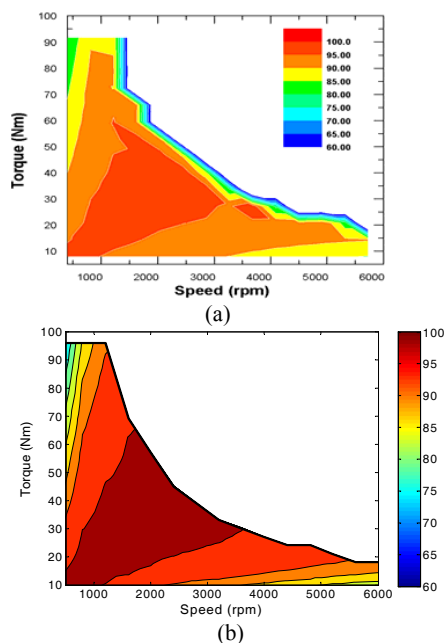Figure 10: Calculated characteristics of motor

(a)

(b)

Figure 11: Efficiency map: (a) calculated efficiency map, (b) measured efficiency map
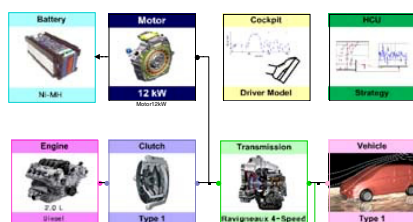

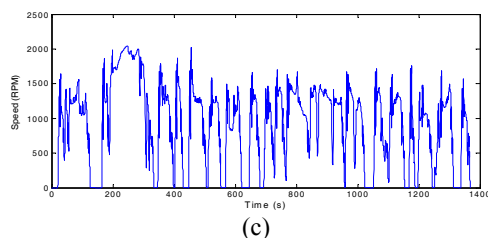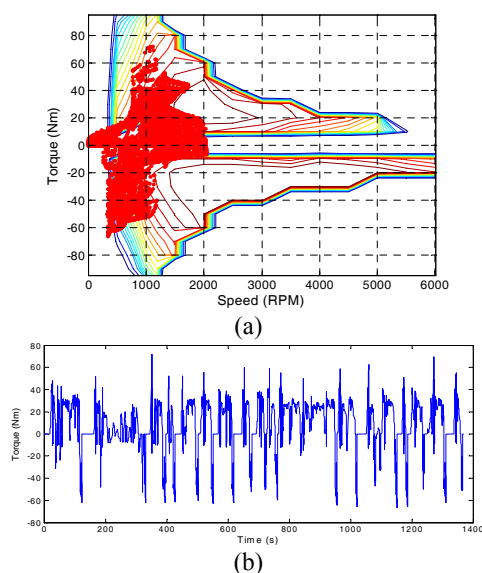Figure 12: HEV simulator for model testing

(a)

(b)

(c)

Figure 13: Results: (a) operating point, (b) motor torque, (c) motor speed

References

[1] S. Williamson, etc., *Comprehensive drivertrain efficiency analysis of Hybrid Electric and Fuel Cell Vehicles based on motor-controller efficiency modelling,* IEEE Transactions on Power Electronics, 2006, (21)730-740

[2] M. Ehsani, etc., *Modern Electric, Hybrid Electric, and Fuel Cell Vehicles*, ISBN 0-8493-3154-4, New York: CRC Press, 2005

[3] S. Morimoto, etc., *Current phase control methods for permanent magnet synchronous motors*, IEEE Transaction on Power Electronics, 1990, (5)133-139

[4] D. M. Ionel, etc., *Computation of core losses in electrical machines using improved models for laminated steel,* IEEE Transactions on Industry Application, 2007, (43)1554-1564

[5] J. W. Jung, etc., *Characteristic Analysis and Comparison of IPMSM for HEV According to Pole and Slot Combination*, Vehicle Power and Propulsion Conference, 2007, 778-783

Authors

Tao Sun is currently pursuing the Ph.D. degree of automotive engineering in Hanyang University, Korea. His interesting research fields are PMSM drive, performance analysis and experiment design.

Soon-O Kwon is currently pursuing the Ph.D. degree of automotive engineering in Hanyang University, Korea. His research interests EPS motor and traction motor design.

Geun-Ho Lee is currently pursuing the Ph.D. degree of automotive engineering in Hanyang University, Korea. He is interested in the motor drive design, and currently researching the low-cost sensor EPS motor drive.

Jung-Pyo Hong received M.S. and Ph.D. degrees in electrical engineering from Hanyang University, Korea, in 1985 and 1995, respectively. Currently he is a professor with department of automotive engineering, Hanyang University. He is interested in the numerical analysis of electro-magnetic field, optimal design, vibration and thermal analysis of electric machinery.